

Electrochemical Impedance Spectroscopy Analysis of 45S5 Bioglass Coating on After Oxidation of CoCrW Alloy

Şükran Merve TÜZEMEN^{1*}, Yusuf Burak BOZKURT¹, Burak ATİK¹, Yakup UZUN¹, Ayhan ÇELİK¹

¹ Atatürk University, Engineering Faculty, Mechanical Engineering Department, Erzurum, Türkiye

Şükran Merve TÜZEMEN ORCID No: 0000-0003-0400-5602

Yusuf Burak BOZKURT ORCID No: 0000-0003-3859-9322

Burak ATİK ORCID No: 0000-0003-2117-9284

Yakup UZUN ORCID No: 0000-0002-5134-7640

Ayhan ÇELİK ORCID No: 0000-0002-8096-0794

*Corresponding author: sukrantuzemen@atauni.edu.tr

(Received: 25.01.2024, Accepted: 24.04.2024, Online Publication: 01.10.2024)

Keywords

Electrochemical
impedance
spectroscopy,
45S5 Bioglass,
Oxidation,
CoCr Alloy

Abstract: Implants and prostheses, which are used to replace a missing or damaged structure in living organisms, must show all the necessary mechanical, tribological, electrochemical and biocompatibility properties together. CoCr alloys are often preferred biomaterials for their good mechanical strength and wear resistance, especially in dental and orthopedic implants. Although these alloys show good corrosion resistance in terms of electrochemical behavior as well as other good properties, when CoCr alloys come into contact with bone tissue, their surfaces show bioinert properties in terms of tissue formation between the implant and bone tissue. Therefore, both their corrosion behavior and biocompatibility properties need to be improved. In this study, CoCrW alloys produced by selective laser melting were coated with commercial 45S5 bioglass powder, a bioactive material, by electrophoretic deposition method. In order to improve the adhesion after coating, CoCrW alloys were subjected to electrochemical etching process during coating. After the coating process was completed, untreated, oxidized, untreated-coated and oxidized-coated samples were examined by electrochemical impedance spectroscopy (EIS) after open circuit potential measurements to investigate their corrosion behavior. As a result of the corrosion tests, it was determined that the oxidized-coated sample showed the best condition compared to the other samples in EIS analyzes.

CoCrW Alaşımının Oksidasyon Sonrasında 45S5 Biyocam Kaplamanın Elektrokimyasal Empedans Spektroskopisi Analizi

Anahtar

Kelimeler

Elektrokimyasal
empedans
spektroskopisi,
45S5 Biyocam,
Oksitleme,
CoCr Alaşımı

Öz: Canlı organizmalarda eksik veya hasarlı bir yapının yerine konulması amacıyla kullanılan implant ve protezlerin gerekli tüm mekanik, tribolojik, elektrokimyasal ve biyouyumluluk özelliklerini bir arada göstermesi gerekir. CoCr alaşımları, özellikle diş ve ortopedik implantlarda iyi mekanik dayanımları ve aşınma dirençleri nedeniyle sıklıkla tercih edilen biyometallerdir. Bu alaşımlar diğer iyi özelliklerinin yanı sıra elektrokimyasal davranış açısından da iyi bir korozyon direnci göstermelerine rağmen, Cr iyonlarının alaşım yüzeyinden bir süre sonra vücuda salındığı tespit edilmiştir. Ayrıca CoCr alaşımları kemik dokusu ile temas ettiğinde yüzeyleri implant ile kemik dokusu arasında doku oluşumu açısından biyo inert özellik göstermektedir. Bu nedenle hem korozyon davranışlarının hem de biyouyumluluk özelliklerinin geliştirilmesi gerekmektedir. Bu çalışmada, seçici lazer eritme ile üretilen CoCrW alaşımları, elektroforetik biriktirme yöntemi ile biyoaktif bir malzeme olan ticari 45S5 biyocam tozu ile kaplanmıştır. Kaplama esnasında adezyonu iyileştirmek için CoCrW alaşımları kaplama öncesi elektrokimyasal oksitleme işlemine tabi tutulmuştur. Kaplama işlemi tamamlandıktan sonra, işlemsiz, oksitlenmiş, işlemsiz-kaplanmış ve oksitlenmiş-kaplanmış numuneler, korozyon davranışlarını araştırmak için açık devre potansiyeli ölçümlerinden sonra elektrokimyasal empedans spektroskopisi (EIS) ile incelenmiştir. Korozyon testlerinden önce kaplamanın yapısal

1. INTRODUCTION

CoCrW alloys, also known as Stellite alloys, are widely used in biomedical, aerospace, space, nuclear and other industries that require superior properties such as high temperature, wear and corrosion resistance [1]. The excellent comprehensive properties of CoCrW alloy are mainly due to the low stacking fault energy of γ -Co, solid solution strengthening of Cr, W and precipitation strengthening of carbide second phase [2,3]. In addition, since these alloys are non-magnetic, radiopaque and MRI compatible, CoCrW alloys are often preferred in hip and knee prostheses and dental implants [4]. The corrosion resistance of CoCr alloys is provided by the passive oxide layer on them as in stainless steels. However, in physiological fluids, factors such as the type and chemical composition of the alloy, exposure time to aggressive ions, pH change and temperature of the biological environment affect the formation and dissolution kinetics of the passive film on CoCr alloys [5,6]. Bone tissue has a piezoelectric behavior that can change the electrochemical potential of metallic implants. These continuous and dynamic processes not only undermine surface performance, but also lead to increased debris in the implant environment. To date, in vivo wear and corrosion and debris generated from articular surfaces have been identified as one of the most important phenomena leading to implant failure [7,8]. On the other hand, some studies have shown that the release of Co^{2+} , Cr^{3+} and Cr^{6+} ions from implants made of CoCr alloys can cause hypersensitivity and inflammatory responses at the implant site [9]. In order to overcome these situations, surface treatments are applied to metallic structures. The film coated with the surface treatment affects the biocompatibility of implant materials and in recent years, bioactive coatings have become more preferred to provide osseointegration as well as corrosion prevention [10].

The electrophoretic deposition (EPD) technique is an electrochemical surface treatment that offers the possibility of coating on complex substrates at room temperature, simple and low installation cost, and the ability to form microstructurally homogeneous films of high purity. The method involves the deposition of colloidal powder particles suspended in suspension onto the substrate by means of an externally applied electric field [11]. Bioactive coatings through the EPD process have been reported in the literature in a few cases and most of the research has focused on high bioactivity hydroxyapatite and bioactive glass coatings [12,13]. The high bioactivity of bioactive glasses (BGs) is based on the release of H^+ ions from the surrounding solution and ions such as Ca^{2+} , Na^+ from the structure as a result of their rapid dissolution. With the release of these ions, a bone-like hydroxyapatite layer forms on the surface of the substrate, so bioactive glasses are preferred in the field of bone tissue repair and reconstruction [14]. Studies show that a strong adhesion is formed in hydroxyapatite-coated structures by the EPD process and that the corrosion resistance of these structures in simulated body fluid

(SBF) is improved compared to untreated samples [15]. However, the application of processes such as pre-coating heat treatment, etching, oxidation has been observed in the literature to increase coating adhesion and give better results in wear and corrosion tests [16].

In addition, CoCr alloys are difficult metallic materials to produce due to their high hardness, melting point and lower ductility [17]. Additive manufacturing (AM) techniques, which have been introduced in recent years with 3D printers, offer a very good solution to fabricate such intricately shaped, difficult-to-produce metallic materials. Among these techniques, selective laser melting (SLM), a powder bed fusion technique, uses computer-aided design (CAD) data to melt metal powders and fuse them layer by layer to form a structure using thermal energy from a focused and accurately controlled laser beam. SLM facilitates the production of complex and non-machinable parts in many industries such as aerospace, aviation, automotive, biomedical and defense industries. Compared to other conventional methods such as weaving and machining, SLM offers advantages such as no casting defects, dimensional accuracy, improved mechanical properties with finer grains due to rapid melting and cooling, lower production cost and less scrap [17,18]. In the literature, the mechanical, tribological and electrochemical properties of many CoCr alloys and composites after additive manufacturing have been investigated in terms of tensile strength, wear and corrosion resistance and it has been observed that they perform better than conventional manufacturing methods [19,20].

In this study, the corrosion resistance of electrochemically oxidized CoCrW alloy coated with 45S5 bioactive glass using EPD technique was analyzed by electrochemical impedance spectroscopy (EIS). The results of untreated, untreated-45S5 coated, oxidized and oxidized-45S5 coated samples were analyzed comparatively in order to observe the improvement of corrosion resistance.

2. MATERIAL AND METHOD

2.1. Materials and Surface Treatments

Samples of CoCrW alloy containing 58.85 wt% Co, 26.30 wt% Cr, 12.62 wt% W, 1.13 wt% Si and 1.1 wt% C were manufactured by the SLM method using a CONCEPT LASER MLab Cusing device with dimensions of $10 \times 10 \times 2 \text{ mm}^3$ and CoCrW powders according to ASTM F75 standard. The manufacturing was carried out using simple straight line scans with 95 W laser power directly directed to melt each layer, a layer thickness of 30 μm and a plane and contour scan speed of 1500 mm/s. After manufacturing, all samples were polished using 80, 220, 400, 800, 1200, 2000 mesh grid with SiC papers and 1 μm grain size with alumina powder respectively, then cleaned with ethanol and dried.

CoCrW alloys prepared to improve adhesion prior to the EPD process were electrochemically oxidized using 1 M H₂SO₄ solution and DC power supply and CoCrW counter electrode for 15 V-10 minutes. For the EPD process, a suspension was prepared by first mixing 99 ml distilled water, 1 ml acetic acid, 0.2 ml phosphate ester and 1 g/L 45S5 Bioglass® (containing 45% SiO₂, 24.5% CaO, 24.5% Na₂O and 6.0% P₂O₅ by weight) commercial powder using a magnetic stirrer for 2 hours. All EPD coating processes were carried out at ambient temperature with a GW GPR-30H10D Laboratory DC Power Supply using graphite as the counter electrode with a distance of approximately 2 cm between them. All samples were coated for 5 minutes at 30 V DC voltage. The phases of the untreated and coated samples were determined by X-Ray Diffraction analysis at 40 kV and 30 mA Cu K α ($\lambda = 1.789 \text{ \AA}$) source diffractometer using XRD-GNR Explorer instrument.

2.2. Electrochemical Impedance Spectroscopy

Untreated, untreated-45S5 coated, oxidized and oxidized-45S5 coated CoCrW samples were subjected to corrosion tests using Gamry G750 Potentiostat/Galvanostat system in stimulated body fluid (SBF) for electrochemical investigation. The test setup was prepared as a triple electrode system using untreated and coated samples as working electrode, graphite rod as counter electrode and Ag/AgCl as reference electrode. The corrosion tests were completed by Open Circuit Potential (OCP) followed by Potentiodynamic Polarization and Electrochemical Impedance Spectroscopy (EIS) analyzes. During the test, the corrosion surface area was set to 0.5 cm² and the time required for the Open Circuit Potential reading was set to 7200 seconds. Potentiodynamic Polarization measurements were performed with a scan rate of 1 mV/s beyond 2 V beyond the Open Circuit Potential values. The Potentiodynamic Polarization and EIS curves obtained from electrochemical analysis were examined in detail.

3. RESULTS

The XRD graph of the untreated, electrochemically oxidized, EPD coated CoCrW alloy samples coated with 45S5 bioglass and duplex (Oxidized+45S5) is given in Figure 1. XRD peaks were obtained in the range of 10°-100° for 2 θ . CoCrW alloy consists of surface-centered cubic (fcc) γ - and hexagonal tight-packed (hcp) ϵ -phase structures [21-23]. XRD diffraction patterns show that CoCrW alloy is composed of fcc γ -phase and hcp ϵ -phase as seen from the peaks obtained at 41°, 43°, 47° and 51° for 2 θ . The presence of Cr₂O₃ phases after the electrochemical oxidation process is seen in the XRD graph given in Figure 1 [24]. In addition, peaks belonging to 45S5 bioglass are seen in the peaks obtained as a result of XRD analysis obtained from bioglass coated surfaces with EPD technique [25].

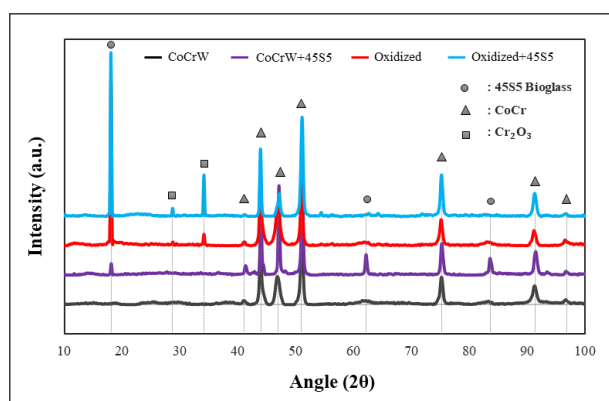


Figure 1. XRD patterns of all samples.

The corrosion behavior of all sample groups subjected to different surface treatments produced by SLM method was carried out by open circuit potential, potentiodynamic polarization and electrochemical impedance spectroscopy measurements in SBF solution at 37°C. Open circuit potential (OCP) measurements were performed for 7200 seconds for all sample groups (Figure 2a). When the OCP graphs are analyzed, it is seen that the curves are directed towards a constant value. The OCP has become stable due to the formation of a stable oxide film on the surface during the OCP measurement and the dissolution and re-formation of this oxide film at the same time [26,27]. It is also seen that the potential of the oxidized surface is higher. Figure 2b shows the potentiodynamic polarization curves for all sample groups at a scan rate of 1 mV/s. The shapes of the potentiodynamic polarization curves are generally similar to each other. Current density, anodic Tafel slope, cathodic Tafel slope, corrosion potential and corrosion rate (E_{corr} , i_{corr} , β_a , β_c , respectively) values of all sample groups were calculated by Tafel extrapolation method and given in Table 1.

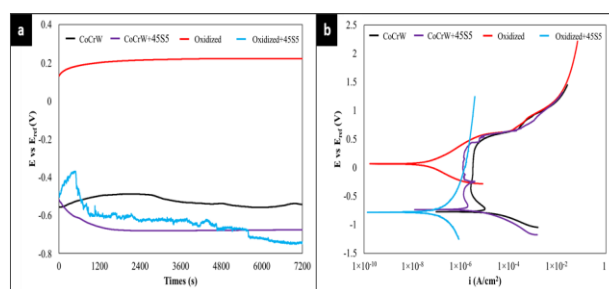


Figure 2. All sample groups (a) OCP and (b) Potentiodynamic polarization graphs.

Corrosion current density (i_{corr}) is an important parameter for the corrosion mechanism. In addition, i_{corr} is directly proportional to the corrosion rate. It can be said that corrosion resistance increases with decreasing current density [27-29]. For this reason, when the i_{corr} values given in Table 1 are examined, it is seen that the i_{corr} values of CoCrW+45S5 ($17.34 \times 10^{-6} \text{ A/cm}^2$), Oxidized ($57.80 \times 10^{-9} \text{ A/cm}^2$) and Oxidized+45S5 ($11.90 \times 10^{-9} \text{ A/cm}^2$) samples are lower than the untreated CoCrW ($195.60 \times 10^{-9} \text{ A/cm}^2$) sample. In addition, the highest corrosion rate was 82.30 mm/year in the untreated sample. This value shows that the untreated CoCrW sample has

lower corrosion resistance compared to the other samples in terms of both mass loss and corrosion rate. In addition, when the potentiodynamic polarization curves of untreated CoCrW and CoCrW+45S5 coated samples are examined, it is seen in Figure 2b that they show a similar passivation feature. This passivation behavior is directly related to the protective passive oxide layer formed on the surface [29].

Table 1. The values of corrosion test results for all samples.

Samples	E _{corr} [mV]	i _{corr} [A/cm ²]	Corrosion Rate [mm/year]
CoCrW	- 56.39	195.60×10 ⁻⁹	82.30
CoCrW+45S5	- 771.50	17.34×10 ⁻⁶	7.296
Oxidized	- 68.50	57.80×10 ⁻⁹	20.59 × 10 ⁻³
Oxidized+45S5	- 779	11.90×10 ⁻⁹	4.229 × 10 ⁻³

Bode and Nyquist curves obtained from electrochemical impedance spectroscopy before potentiodynamics in SBF solution for all sample groups are given in Figure 3 and Figure 4. Phase angle is directly proportional to corrosion. The probability of corrosion decreases with increasing phase angle [29]. In bode and nyquist curves, corrosion resistance increases with the increase of capacitive semicircle diameter [27]. Thus, when the bode curves obtained are examined, it is seen that the Oxidized + 45S5 duplex surface treated sample has high corrosion resistance.

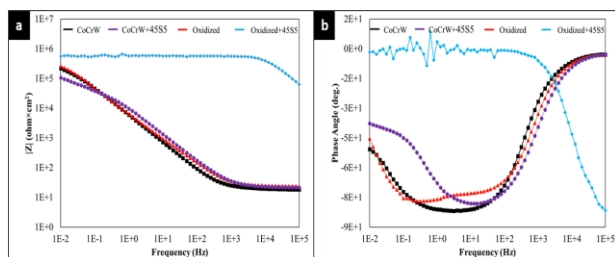


Figure 3. Bode curves for all sample groups (a) Frequency-|Z| and (b) Frequency-Phase angle curves.

It means that the corrosion resistance increases as the capacitive loop expands in Nyquist curves. Looking at the Nyquist curves given in Figure 4, it is seen that the capacitive semicircle diameter of the Oxidized+45S5 sample is considerably higher compared to the other samples. This shows that it has the highest corrosion resistance compared to other samples.

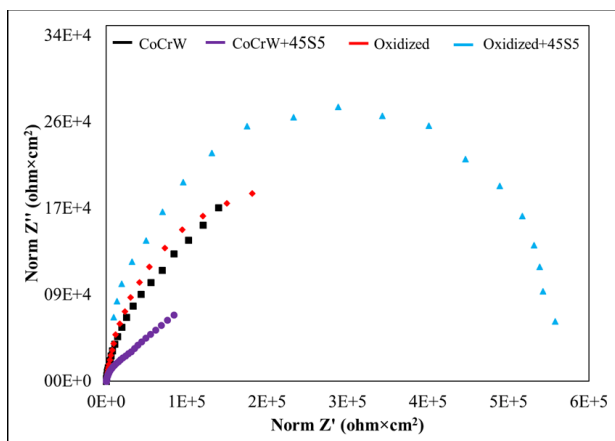


Figure 4. Nyquist curves for all samples groups

4. DISCUSSION AND CONCLUSION

Electrochemical oxidation, 45S5 Bioglass and duplex (oxidation+45S5 Bioglass) coating processes were carried out on CoCrW alloy produced by SLM. Electrochemical corrosion properties of untreated and coated surfaces were investigated in SBF solution and the results obtained are summarized below:

- ✓ According to XRD results, CoCr, Cr₂O₃ and 45S5 Bioglass peaks were obtained. In addition, fcc γ -phase and hcp ϵ -phases of untreated CoCrW alloy were found.
- ✓ In the electrochemical corrosion test results carried out in SBF solution, the highest corrosion resistance was observed on the Oxidized+45S5 coated surface with 11.90×10^{-9} A/cm² i_{corr} value.
- ✓ The electrochemical corrosion performances of CoCrW+45S5, oxidation and oxidation+45S5 coatings on the surface of CoCrW alloy produced by SLM technique have been improved.

Acknowledgement

This study was presented as an oral presentation at the "6th International Conference on Life and Engineering Sciences (ICOLES 2023)" conference.

REFERENCES

- [1] Kuzucu V, Ceylan M, Çelik H, Aksoy I. Microstructure and phase analyses of Stellite 6 plus 6 wt.% Mo alloy. *Journal of Materials Processing Technology*. 1997; 69(1–3): 257-263.
- [2] Tian LY, Lizárraga R, Larsson H, Holmström E, Vitos L. A first principles study of the stacking fault energies for fcc Co-based binary alloys. *Acta Materialia*. 2017; 136: 215-223.
- [3] Wang S, Zhan S, Hou X, Wang L, Zhang H, Zhang H, Sun Y, Huang L. Microstructure and Mechanical Property of a Multi-Scale Carbide Reinforced Co–Cr–W Matrix Composites. *Crystals*. 2022; 12(2):198.
- [4] Yan Y, Neville A, Dowson D. Tribo-corrosion properties of cobalt-based medical implant alloys in simulated biological environments. *Wear*. 2007; 263(7–12): 1105-1111.
- [5] Ouerd A, Alemany-Dumont C, Normand B, Szunerits S. Reactivity of CoCrMo alloy in physiological medium: Electrochemical characterization of the metal/protein interface. *Electrochimica Acta*. 2008; 53(13): 4461-4469.
- [6] Igual Muñoz A, Mischler S. Interactive Effects of Albumin and Phosphate Ions on the Corrosion of CoCrMo Implant Alloy. *J. Electrochem. Soc.* 2007; 154: 10.
- [7] Gittens RA, Olivares-Navarrete R, Tannenbaum R, Boyan BD, Schwartz Z. Electrical Implications of Corrosion for Osseointegration of Titanium Implants. *Journal of Dental Research*. 2011; 90(12): 1389-1397.

- [8] Diaz I, Martinez-Lerma JF, Montoya R, Llorente I, Escudero ML, García-Alonso MC. Study of overall and local electrochemical responses of oxide films grown on CoCr alloy under biological environments. *Bioelectrochemistry*. 2017; 115: 1-10.
- [9] Mani G. *Metallic biomaterials: cobalt-chromium alloys*. Murphy W, Black J, Hastings G. (Eds.), *Handb. Biomater. Prop* (second ed.). 159-166, 2016, Springer.
- [10] Chen Q, Thouas GA. *Metallic implant biomaterials*. *Mater Sci Eng R Rep*. 2015; 87: 1-57.
- [11] Boccaccini AR, Peters C, Roether JA, Eifler D, Misra SK, Minay EJ. Electrophoretic deposition of polyetheretherketone (PEEK) and PEEK/Bioglass® coatings on NiTi shape memory alloy wires. *J. Mater. Sci*. 2006; 41: 8152-8159.
- [12] Pishbin F, Simchi A, Ryan MP, Boccaccini AR. Electrophoretic deposition of chitosan/45S5 Bioglass® composite coatings for orthopaedic applications. *Surf. Coatings Technol*. 2011; 205: 5260-5268.
- [13] Khanmohammadi S, Ojaghi-Ilkhchi M, Farrokhi-Rad M. Evaluation of Bioactive glass and hydroxyapatite based nanocomposite coatings obtained by electrophoretic deposition. *Ceramics International*. 2020; 46: 26069-26077.
- [14] Vichery C, Nedelec J-M. *Bioactive Glass Nanoparticles: From Synthesis to Materials Design for Biomedical Applications*. *Materials*. 2016; 9(4): 288.
- [15] Khanmohammadi S, Ojaghi-Ilkhchi M, Khalil-Allafi J. Electrophoretic deposition and characterization of Bioactive glass-whisker hydroxyapatite nanocomposite coatings on titanium substrate. *Surface and Coatings Technology*. 2019; 378: 1-13.
- [16] Pawlik A, Rehman MAU, Nawaz Q, Bastan FE, Sulka GD, Boccaccini AR. Fabrication and characterization of electrophoretically deposited chitosan-hydroxyapatite composite coatings on anodic titanium dioxide layers. *Electrochim. Acta*. 2019; 307: 465-473.
- [17] Ozel T, Bartolo P, Ceretti E, De Ciurana Gay J, Rodriguez CA, Da Silva JVL. *Biomedical devices: design, prototyping and manufacturing*. 2017, John Wiley & Sons.
- [18] Takaichi A, Suyalatu T, Nakamoto N, Joko N, Nomura Y, Tsutsumi S. Microstructures and mechanical properties of Co-29Cr-6Mo alloy fabricated by selective laser melting process for dental applications. *J Mech Behav Biomed Mater*. 2013; 21: 67-76.
- [19] Mergulhão MV, Podestá CE, das Neves MDM. Valuation of mechanical properties and microstructural characterization of ASTM F75 Co-Cr alloy obtained by Selective Laser Melting (SLM) and casting techniques. *Mater Sci Forum*. 2017; 899: 323-328.
- [20] Seyedi M, Zanotto F, Monticelli C, Balbo A, Liverani E, Fortunato A. Microstructural characterization and corrosion behaviour of SLM CoCrMo alloy in simulated body fluid. *Metall Ital*. 2018; 110: 45-50.
- [21] Lee HW, Jung K-H, Hwang S-K, Kang S-H, Kim D-K. Microstructure and mechanical anisotropy of CoCrW alloy processed by selective laser melting. *Materials Science and Engineering: A*. 2019; 749: 65-73.
- [22] Lu Y, Wu S, Gan Y, Zhang S, Guo S, Lin J, Lin J. Microstructure, mechanical property and metal release of As-SLM CoCrW alloy under different solution treatment conditions. *Journal of the Mechanical Behavior of Biomedical Materials*. 2016; 55: 179-190.
- [23] Luo J, Wu S, Lu Y et al. The effect of 3 wt.% Cu addition on the microstructure, tribological property and corrosion resistance of CoCrW alloys fabricated by selective laser melting. *J Mater Sci: Mater Med*. 2018; 29(37).
- [24] Lu Y, Lin W, Xie M, Xu W, Liu Y, Lin J, Yu C, Tang K, Liu W, Yang K, Lin J. Examining Cu content contribution to changes in oxide layer formed on selective-laser-melted CoCrW alloys. *Applied Surface Science*. 2019; 464: 262-272.
- [25] Azzouz I, Faure J, Khelifi K, Cheikh Larbi A, Benhayoune H. Electrophoretic Deposition of 45S5 Bioglass® Coatings on the Ti6Al4V Prosthetic Alloy with Improved Mechanical Properties. *Coatings*. 2020; 10(12):1192.
- [26] Qin P, Chen LY, Liu YJ, Zhao CH, Lu YJ, Sun H, Zhang LC. Corrosion behavior and mechanism of laser powder bed fusion produced CoCrW in an acidic NaCl solution. *Corrosion Science*. 2023; 213: 110999.
- [27] Uzun Y., Taş B., Tüzemen Ş.M., Çelik A. The Improvement of Corrosion Performance of CoCrW Alloy with Bioglass Coating. 3rd International Natural Science, Engineering and Materials Technology Conference, NEM 2023. Gazimagusa, Cyprus (Kktc); 2023. p.182-189.
- [28] Lu Y, Ren L, Xu X, Yang Y, Wu S, Luo J, Yang M, Liu L, Zhuang D, Yang K, Lin J. Effect of Cu on microstructure, mechanical properties, corrosion resistance and cytotoxicity of CoCrW alloy fabricated by selective laser melting. *Journal of the Mechanical Behavior of Biomedical Materials*. 2018; 81: 130-141.
- [29] Lu Y, Wu S, Gan Y, Li J, Zhao C, Zhuo D, Lin J. Investigation on the microstructure, mechanical property and corrosion behavior of the selective laser melted CoCrW alloy for dental application. *Materials Science and Engineering: C*. 2015; 49: 517-525.
- [30] Sun D, Wharton JA, Wood RJK, Ma L, Rainforth WM. Microabrasion–corrosion of cast CoCrMo alloy in simulated body fluids. *Tribology International*. 2009; 42(1): 99-110.